Overexpression of hsa_circ_0001861 inhibits pulmonary fibrosis through targeting miR-296-5p/BCL-2 binding component 3 axis

Tao Wu, Shikui Wu, Hailu Jiao, Jun Feng, Xiang Zeng

Department of Respiratory and Critical Care Medicine, First Affiliated Hospital of Hunan Provincial College of Traditional Chinese Medicine, Zhuzhou, Hunan, China

ABSTRACT

Pulmonary fibrosis is a progressive lung disorder. Evidence has shown that hsa_circular (circ)RNA_0001861 is dysregulated in pulmonary fibrosis. However, the detailed function of hsa_circRNA_0001861 in pulmonary fibrosis remains unexplored. To investigate the function of hsa_circRNA_0001861 in pulmonary fibrosis, human pulmonary fibroblasts *in vitro* were used, and cell counting kit-8 (CCK-8) and 5-ethynyl-2'-deoxyuridine (EdU) staining were performed to assess cell viability and proliferation, respectively. Western blot analysis and reverse transcription-quantitative PCR (RT-qPCR) were used to evaluate protein and mRNA levels. Meanwhile, the relationship among hsa_circRNA_0001861, miR-296-5p and BCL-2 binding component 3 (BBC3) was investigated by RNA pull-down assays. Furthermore, an *in vivo* model of lung fibrosis was constructed to assess the function of hsa_circRNA_0001861 in lung fibrosis. The data revealed that TGF-β1 significantly increased the proliferation of pulmonary fibroblasts, while this phenomenon was markedly abolished by hsa_circRNA_0001861 overexpression. hsa_circRNA_0001861 overexpression markedly inhibited TGF-β1−induced fibrosis in pulmonary fibroblasts through the mediation of α-smooth muscle actin, E-cadherin, collagen III and fibronectin 1. Meanwhile, hsa_circRNA_0001861 could bind with miR-296-5p, and BBC3 was identified to be the downstream mRNA of miR-296-5p. In addition, the upregulation of hsa_circRNA_0001861 clearly reversed TGF-β1−induced fibrosis and proliferation in pulmonary fibroblasts through the upregulation of BBC3. Furthermore, hsa_circRNA_0001861 upregulation markedly alleviated pulmonary fibrosis *in vivo*. Hsa_circRNA_0001861 upregulation attenuated pulmonary fibrosis by modulating the miR-296-5p/BBC3 axis. Hence, the present study may provide some insights for the discovery of new methods against pulmonary fibrosis.

Key words: pulmonary fibrosis; hsa_circRNA_0001861; BBC3; miR-296-5p.

Correspondence: Tao Wu, Department of Respiratory and Critical Care Medicine, First Affiliated Hospital of Hunan Provincial College of Traditional Chinese Medicine, No. 571 Renmin Middle Road, Zhuzhou 412000, Hunan, China. E-mail: wutao_wt04@163.com

Contributions: TW, study supervision, experiments design; TW, SW, HJ, experiments performing; HJ, JF, raw data checking; TW, JF, manuscript drafting; XZ, manuscript review and revision. All the authors read and approved the final version of the manuscript and agreed to be accountable for all aspects of the work.

Conflict of interest: the authors declare that they have no competing interests, and all authors confirm accuracy.

Ethics approval: the Ethics Committee of the First Affiliated Hospital of Hunan Provincial College of Traditional Chinese Medicine approved this study (approval no. 20210903).

Availability of data and materials: all data generated or analyzed during this study are included in this article and the raw data could be made available from the corresponding author on reasonable request.

Introduction

Pulmonary fibrosis is a subtype of progressive and chronic lung-related disease.[1] Pulmonary fibrosis includes hypersensitivity pneumonitis, sarcoidosis, pulmonary fibrosis and radiation-induced fibrosis.[2,3] Pulmonary fibrosis is the most severe lung condition, causing lung function decline, lung parenchyma fibrosis, respiratory failure and the progression of pulmonary fibrosis, which can in turn lead to mortality.[4] In addition, it has been shown that environmental exposure, cigarette smoking, viral infection and exposure to occupational hazards could cause the occurrence of pulmonary fibrosis.[5-7] Drug administration is the main treatment method against pulmonary fibrosis, with the outcomes remaining unfavorable.[8] Therefore, it is essential to explore new strategies against pulmonary fibrosis.

Recently, the reports on new biomarkers (*e.g.*, mRNAs and miRNAs) related to the progression of pulmonary fibrosis have been increasing.[9-11] For example, glycoprotein Krebs von den Lungen-6, chemokine (C-C motif) ligand 18, surfactant protein-D and matrix metalloproteinase-1 could act as the diagnostic biomarkers for pulmonary fibrosis;[12,13] meanwhile, circular RNAs (circRNAs) are non-coding RNAs with a closed structure, mainly distributed in the cytoplasm.[14] It has been reported that circRNAs participate in the regulation of gene expression.[15] CircRNAs could regulate parental gene levels by modulating RNA transcript activity.[16] In addition, circRNAs participated in progression of pulmonary fibrosis.[17] A previous study indicated that hsa_circ_0001861 level was downregulated in patients with pulmonary fibrosis, suggesting hsa_circ_0001861 might have potential in treatment of pulmonary fibrosis.[18] However, the detailed function of hsa_circ_0001861 in pulmonary fibrosis remains unknown.

Based on the above data, we hypothesized that hsa_circ_0001861 might inhibit the progression of pulmonary fibrosis. Therefore, the aim of the present study was to assess the function of hsa_circ_0001861 on pulmonary fibroblast growth. This study may provide new insights to assist the discovery of new strategies for the treatment of pulmonary fibrosis.

Materials and Methods

Cell culture

Human pulmonary fibroblasts were obtained from Procell Life Science & Technology Co., Ltd. (Wuhan, China), and 293T cells were purchased form American Type Culture Collection. Pulmonary fibroblasts were maintained in DMEM containing FBS (10%), penicillin (100 U/mL) and streptomycin (100 μg/mL) at 37°C with 5% CO_2. To mimic pulmonary fibrosis *in vitro*, cells were exposed to TGF-β (5 ng/mL; R&D system, No. 7754-BH) for 48 h as previously described.[19]

Cell transfection

cDNA oligonucleotides inhibiting the BCL-2 binding component 3 (BBC3) level were cloned into the pLVX-shRNA (BBC3 shRNA). Next, BBC3 shRNA plasmids were transfected into 293T cells. The supernatant was collected at 48 h. BBC3 shRNA supernatants were then infected into fibroblasts. Subsequently, puromycin (2.5 μg/mL; No. A1113802; Gibco, Waltham, MA, USA) was used to select the transfected cells. The sequences for shRNAs were as follows:
BBC3 shRNA: 5'-ACGACCTCAACGCGCAGTA-3';
NC shRNA: 5'-UCUCCGAACGUGUCACGU-3'.

For hsa_circ_0001861 overexpression, pcDNA3.1-hsa_circ_0001861 (hsa_circ_0001861 OE) or pcDNA3.1 (NC) was applied to transfect the cells for 48 h, according to the manufacturer's instructions. The procedure was performed as previously described.[20]

Reverse transcription-quantitative PCR (RT-qPCR)

TRIzol (Takara Bio, Inc.) was used to extract total RNA. Next, the EntiLink™ Kit (ELK Biotechnology, Co. Ltd., No. EQ003) was used for RT into cDNA, according to the manufacturer's instructions. Regarding as RT for miR-296-5p and U6, stem loop RT primers are needed. The primers were obtained from ELK Biotechnology, Co. Ltd. and listed as follows:
miR-296-5p: 5'-CTCAACTGGTGTCGTGGAGTCGGCAATTCAGTTGAGACAGGATT-3';
U6: 5'-AACGCTTCACGAATTTGCGT-3'.

SYBR Green was used in RT-qPCR analysis using Agilent System (Agilent Technologies, Inc.). The following thermocycling conditions were used for the qPCR: Initial denaturation at 95°C for 5 min; followed by 40 cycles of 95°C for 10 sec, 60°C for 30 sec and 72°C for 30 sec. The primers were obtained from Genepharma and listed as follows:
miR-296-5p: forward 5'-TTAGGGCCCCCCCTCA-3' and reverse 5'-CTCAACTGGTGTCGTGGAGTC-3';
Hsa_circ_0001861: forward 5'-TGATTCGTAGTGGGATCCGAG-3' and reverse 5'-CAGCATCCAGGATCCTCTTGT-3';
BBC3, forward 5'-GGACGACCTCAACGCACAGTA-3' and reverse 5'-AGGGTGTCAGGAGGTGGGAG-3';
β-actin: forward 5'-GTCCACCGCAAATGCTTCTA-3' and reverse 5'-TGCTGTCACCTTCACCGTTC-3';
U6: forward 5'-CTCGCTTCGGCAGCACAT-3' and reverse 5'-AACGCTTCACGAATTTGCGT-3'.

The $2^{-\Delta\Delta t}$ method was used to quantify the data.[21] β-Actin or U6 was used for normalization.

Cell counting kit (CCK-8) assay

Pulmonary fibroblasts (10,000 cells/well) were cultured in a 24-well plate overnight. Next, cells were exposed to TGF-β1, TGF-β1 + NC or TGF-β + hsa_circ_0001861 OE for 24, 48 or 72 h. Next, CCK-8 (10 μL; no. C0038; Beyotime Institute of Biotechnology, Shanghai, China) was added into each well. Following incubation for 2 h, a microplate reader (DR-200Bs, Wuxi Hiwell-Diatek Instruments Co., Ltd., Wuxi, China) was used to measure absorbance (450 nm). The procedure was performed as previously described.[22]

5-ethynyl-2'-deoxyuridine (EDU) staining

In this study, cell proliferation was measured with an EdU cell proliferation kit (Guangzhou RiboBio Co., Ltd., Guangzhou, China; no. C10310-1). Briefly, 2×10^4 cells were fixed with 4% paraformaldehyde for 30 min at room temperature, and then incubated with EdU (5 μM) reagent for 2 h, followed by incubation with Apollo dye solution in the dark for 30 min. After that, 4',6-Diamidino-2-phenylindole (DAPI) was used for staining the nucleus for 5 min, and a fluorescence microscope (Olympus Co., Tokyo, Japan; IX51, light: mercury lamp, objective: 20x) was used to observe the data. The procedure was performed as previously described.[23]

Dual luciferase assay

The wild-type (WT) and mutant (MUT) hsa_circ_0001861/BBC3 were sub-cloned into the vectors (pmiR-RB-Report™; Guangzhou RiboBio Co., Ltd.). Lipofectamine® 2000 (Invitrogen; Thermo Fisher Scientific, Inc., Waltham, MA, USA) was used to transfect the cells together with miR-296-5p

agomir (Guangzhou RiboBio Co., Ltd.), control vector and the WT- or MUT-hsa_circ_0001861 plasmid for 48 h, according to the manufacturer's instructions. A Dual-luciferase System (Promega Co., Madison, WI, USA) was used to evaluate the luciferase activity. The procedure was performed as previously described.[24] The sequences for miRNAs were listed as follows:
miR-296-5p agomir: 5'-AGGGCCCCCCCUCAAUCCUGU-3';
miR-NC: 5'-ACTGGAGACACGTGCACTGTAGA-3'.

RNA pull-down

The biotinylated hsa_circ_0001861 and bio-ctrl originated from GenePharma Co., Ltd. (Shanghai, China), and streptavidin-conjugated magnetic beads were used to coat them. Cells were lysed, and magnetic beads were used to incubate the cells for 6 h. The RNA was extracted, and RT-qPCR was used to assess the enrichment of miR-296-5p. The procedure was performed as previously described.[24]

Wound healing assay

Pulmonary fibroblasts ($5x10^5$ cells) were plated into 6-well plates and incubated overnight. A pipette tip (200 µL) was used to make the wound across the monolayered cells. The suspension cells were incubated in DMEM without FBS after being washed twice with PBS. pcDNA3.1-hsa_circ_0001861 was used to transfect the cells. A light microscope (IX51, objective: 20x; Olympus Co.) was used to monitor the wound. The wound was observed regularly and imaged after 48 h. ImageJ software (National Institutes of Health) was used to assess cell migration area as previously described.[25] Wound healing rate (%) = (migration distance/original distance) ×100. Migration distance was the difference between the width of the wound at 0 h and 48 h, while original distance was the width of the wound at 0 h.

TUNEL staining

Pulmonary fibroblasts were fixed with 4% paraformaldehyde for 20 min and then permeabilized with 0.1% Triton X-100 for 10 min. Next, cells were stained with TUNEL reagent A and B (cat. no. 11684817910; Roche, Basel, Switzerland) for 1 h at 37°C in darkness. The nucleus was counterstained with DAPI for 20 min in darkness. Finally, images were observed under a fluorescence microscope (IX51; Olympus Co.) and the apoptotic cells were analyzed using the Image-Pro Plus software (Media Cybernetics, Rockville, MD, USA).

Western blot assay

Radioimmunoprecipitation assay buffer (Beyotime Institute of Biotechnology) was used for protein isolation, and bicinchoninic acid assay kit (Beyotime Institute of Biotechnology) was performed to quantify the proteins.[26] Subsequently, proteins were separated on an SDS gel (10%) and then transferred onto PVDF membranes (Invitrogen; Thermo Fisher Scientific, Inc.). Following blocking with 5% skimmed milk, membranes were incubated with primary antibodies against α-smooth muscle actin (α-SMA; cat. No. ab108531; dilution, 1:1,000; Abcam, Cambridge, UK), E-cadherin (cat. no. ab40772; dilution, 1:1,000; Abcam), collagen III (cat. no. ab184993; dilution, 1:1,000, Abcam), β-actin (cat. no. ab8226; dilution, 1:1,000; Abcam) and fibronectin 1 (cat. no. ab2413; dilution, 1:1,000; Abcam). Next, membranes were incubated with HRP-conjugated secondary antibodies for 1 h (cat. no. ab288151; Abcam; 1:5,000). An enhanced chemiluminescence detection kit (cat. no. NCI5079; Thermo Fisher Scientific, Inc.) was used to assess the immunoreactive signals. The AlphaEaseFC software (Alpha Innotech, San Leandro, CA, USA) was used to analyze the intensity of each band. β-Actin was considered as the internal control.

Animal study

Male C57BL/6 mice (n=20; 18-22 g, 9-12 weeks) originated from Vital River Laboratories, Ltd. (Beijing, China) and placed in SPF conditions, following the guidelines of ARRIVE (https://arriveguidelines.org/). The present was approved by the Ethics Committee of the First Affiliated Hospital of Hunan Provincial College of Traditional Chinese Medicine (approval no., 20210903). Bleomycin was used to induce pulmonary fibrosis *in vivo*.[27] The animals were divided into the control, bleomycin (BLM), hsa_circ_0001861 OE and BLM + hsa_circ_0001861 OE groups. Pentobarbital (1%; 40 mg/kg) was used 1% to anesthetize mice by intraperitoneal injection. Afterwards, mice in the BLM and BLM + hsa_circ_0001861 OE groups were administered using sterile saline containing BLM *via* intratracheal injection (50 µL; 1 unit/kg). Meanwhile, mice were treated with either lentivirus particles overexpressing hsa_circ_0001861 *via* intratracheal injection ($1x10^{11}$ vector) following BLM administration for 3 days.[28] Finally, the animals were killed using CO_2 (took place in 2021), and animal death was confirmed by heartbeat and respiration (> 3 min) at a displacement rate of 40% of the chamber volume/min.

Immunohistochemical staining

4% paraformaldehyde overnight at 4°C was used to fix the tissues, which were then paraffin-embedded and cut into 5-µm-thick sections. Next, anti-collagen I (cat. no ab138492; 1:200; Abcam) and anti-α-SMA (cat.no ab124964; 1:200, Abcam) primary antibodies were used to label the samples overnight at 4□, and then the sections were probed with a secondary antibody (cat. no AS-1107; Aspen Biosciences, San Diego, CA, USA) for 50 min at 37°C. A light microscope (IX51, objective: 20x; Olympus Co.) was used to observe the data, and the results were analyzed by Image-Pro Plus software. The procedure was in accordance with the previous report.[29] Sections processed without the primary antibodies were set as negative controls.

Histology and fibrosis analysis

To fix the tissues overnight, 4% paraformaldehyde was used, then tissues were paraffin-embedded and cut into 5-µm-thick sections.[30] Subsequently, the sections were routinely stained with hematoxylin and eosin (H&E); to determine the degree of lung fibrosis, Masson's trichrome staining was performed. The slides were observed using a light microscope (IX5; Olympus Co.), and the fibrosis area was measured by the Image-Pro Plus software.

Statistical analysis

Each experiment was repeated in triplicate. The data are expressed as the mean ± SD. GraphPad Prism software (version 7.0) was used in data analysis. ANOVA and Tukey's tests were carried out for multiple group comparisons. A p-value <0.05 were considered to indicate a statistically significant difference.

Results

Hsa_circ_0001861 overexpression reverses TGF-β-mediated fibroblast function

It was reported that TGF-β was considered as a vital factor in progression of fibrosis.[31] Thus, to assess the role of hsa_circ_0001861 in pulmonary fibrosis, pulmonary fibroblasts were treated with 5 ng/mL TGF-β. As shown in Figure 1A, the level of hsa_circ_0001861 in pulmonary fibroblasts was decreased by TGF-β, and the level of hsa_circ_0001861 was markedly increased by pcDNA3.1-hsa_circ_0001861 in pulmonary fibrob-

lasts (Figure 1B). TGF-β significantly increased the viability of pulmonary fibroblasts, while the overexpression of hsa_circ_0001861 reversed this phenomenon (Figure 1C). Consistently, TGF-β-induced fibroblast proliferation was markedly restored by hsa_circ_0001861 upregulation (Figure 1D). In combination, these findings showed that hsa_circ_0001861 overexpression reversed TGF-β-induced migration in fibroblasts.

Hsa_circ_0001861 overexpression restores TGF-β-induced upregulation of fibrotic proteins

To evaluate the function of hsa_circ_0001861 in pulmonary fibrosis, wound healing was performed to assess cell migration. As indicated in Figure 2A, TGF-β-induced fibroblast migration was markedly restored by hsa_circ_0001861 upregulation. TGF-β reduced the level of E-cadherin, but elevated the levels of collagen I, α-SMA and fibronectin in fibroblasts, while this phenomenon was restored by hsa_circ_0001861 overexpression (Figure 2 B-F). In conclusion, hsa_circ_0001861 overexpression restored the TGF-β-induced upregulation of fibrotic proteins.

Hsa_circ_0001861 binds to miR-296-5p

To validate the target miRNA of hsa_circ_0001861, the starBase database (https://starbase.sysu.edu.cn/index.php) was used. In Figure 3A, miR-296-5p was predicted to be targeted by hsa_circ_0001861. The luciferase activity in WT-hsa_circ_0001861 was markedly decreased by miR-296-5p agomir, while hsa_circ_0001861 did not affect the luciferase activity in MT-hsa_circ_0001861 (Figure 3B). The enrichment of miR-296-3p was upregulated by probe-hsa_circ_0001861 (Figure 3C). Meanwhile, it has been reported that excessive proliferation of pulmonary fibroblasts could contribute to the occurrence and progression of lung fibrosis.[32] Among the downstream targets of miR-296-3p, BBC3 upregulation could inhibit cell proliferation.[33] Thus, it could be hypothesized that hsa_circ_0001861 might inhibit the pulmonary fibrosis through mediation of miR-296-3p/BBC3 axis. BBC3 was identified as the downstream target of miR-296-5p (Figure 4A). miR-296-5p upregulation markedly inhibited the luciferase activity in WT-BBC3 (Figure 4B). Furthermore, the level of BBC3 in fibroblasts was markedly increased by hsa_circ_0001861 overexpression (Figure 4C). In conclusion, hsa_circ_0001861 bound to miR-296-5p.

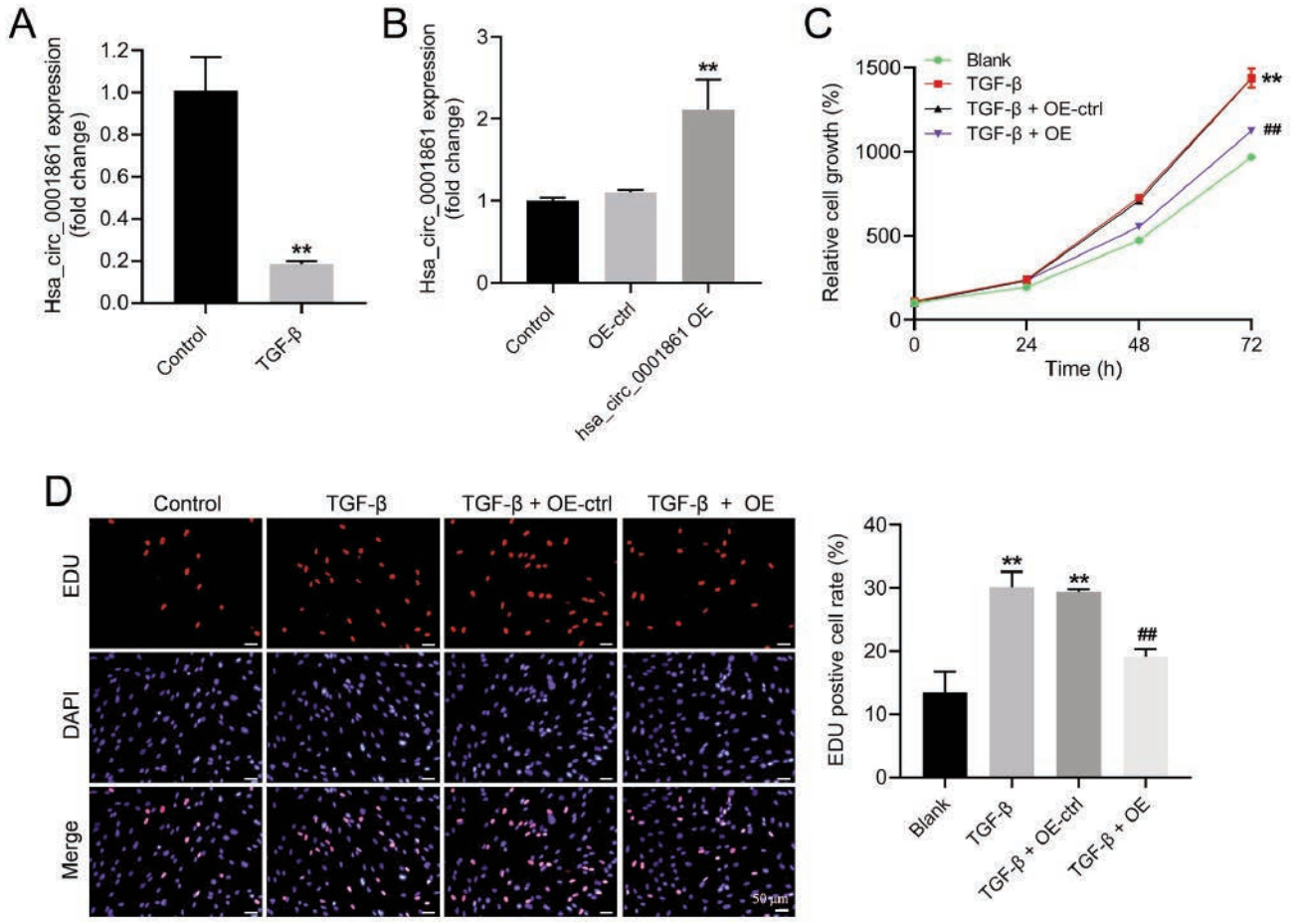

Figure 1. Hsa_circ_0001861 overexpression reversed TGF-β-mediated fibroblast function. **A**) Pulmonary fibroblasts were exposed to TGF-β (5 ng/mL); the level of hsa_circ_0001861 in pulmonary fibroblasts was investigated by RT-qPCR. **B**) Pulmonary fibroblasts were transfected with pcDNA3.1-hsa_circ_0001861 or pcDNA3.1 for 48 h; the level of hsa_circ_0001861 in pulmonary fibroblasts was investigated by RT-qPCR. **C**) Pulmonary fibroblasts were treated with TGF-β, TGF-β + pcDNA3.1 or TGF-β + pcDNA3.1-hsa_circ_0001861; the viability of pulmonary fibroblasts was assessed by CCK8 assay. **D**) The proliferation of pulmonary fibroblasts was tested by EdU staining. **p<0.01 compared to control; ##p<0.01 compared to TGF-β.

Hsa_circ_0001861 overexpression restores TGF-β-induced proliferation and fibrosis in fibroblasts through BBC3 upregulation

To further confirm the mechanism underlying the function of hsa_circ_0001861 in fibroblasts, fibroblasts were transfected with BBC3 shRNA. As shown in Figure 5A, the level of BBC3 in fibroblasts was significantly downregulated by BBC3 shRNA. The inhibitory effect of hsa_circ_0001861 on the proliferation of TGF-β-treated fibroblasts was significantly rescued by BBC3 knockdown (Figure 5B). Meanwhile, TGF-β elevated the levels of α-SMA and collagen I in fibroblasts, which was partially rescued by pcDNA3.1-hsa_circ_0001861 (Figure 5 C-E). By contrast, BBC3 knockdown could significantly aggravate the TGF-β-induced upregulation of collagen I and α-SMA (Figure 5 C-E). The effect of hsa_circ_0001861 overexpression on these proteins was abolished by BBC3 shRNA (Figure 5 C-E). Furthermore, the upregulation of hsa_circ_0001861 markedly induced the apoptosis of TGF-β-treated fibroblasts, while the apoptotic effect of hsa_circ_0001861 was markedly rescued by BBC3 shRNA (Figure 6 A,B). In conclusion, hsa_circ_0001861 overexpression restored TGF-β-induced proliferation and fibrosis in fibroblasts through BBC3 upregulation.

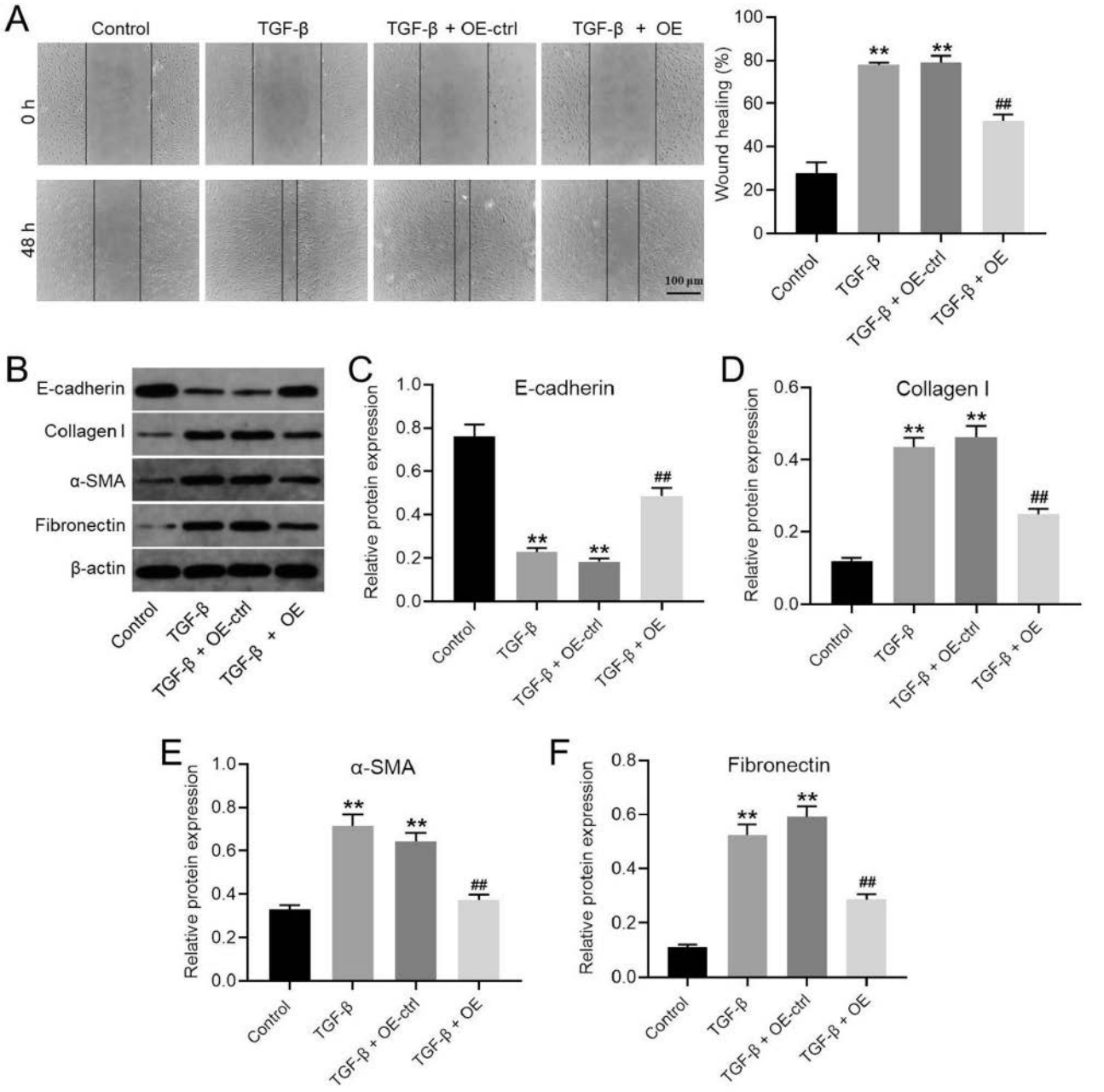

Figure 2. Hsa_circ_0001861 overexpression restored TGF-β-induced upregulation of fibrotic proteins. **A**) Pulmonary fibroblast migration was assessed by wound healing assay. **B-F**) The protein levels of α-SMA, collagen I, E-cadherin and fibronectin in pulmonary fibroblasts were assessed by Western blot. **p<0.01 compared to control; ##p<0.01 compared to TGF-β.

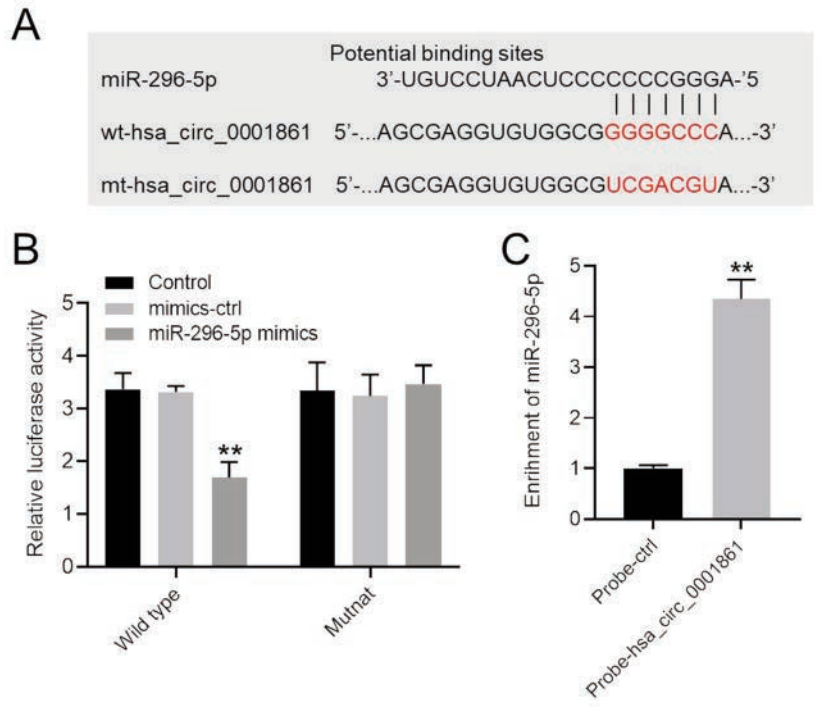

Figure 3. Hsa_circ_0001861 bound with miR-296-5p. **A**) Starbase was applied for predicting the downstream of hsa_circ_0001861. **B**) The luciferase activity was assessed by dual luciferase activity. **C**) The enrichment of miR-296-5p in pulmonary fibroblasts was assessed by RNA pull-down. **p<0.01 compared to control.

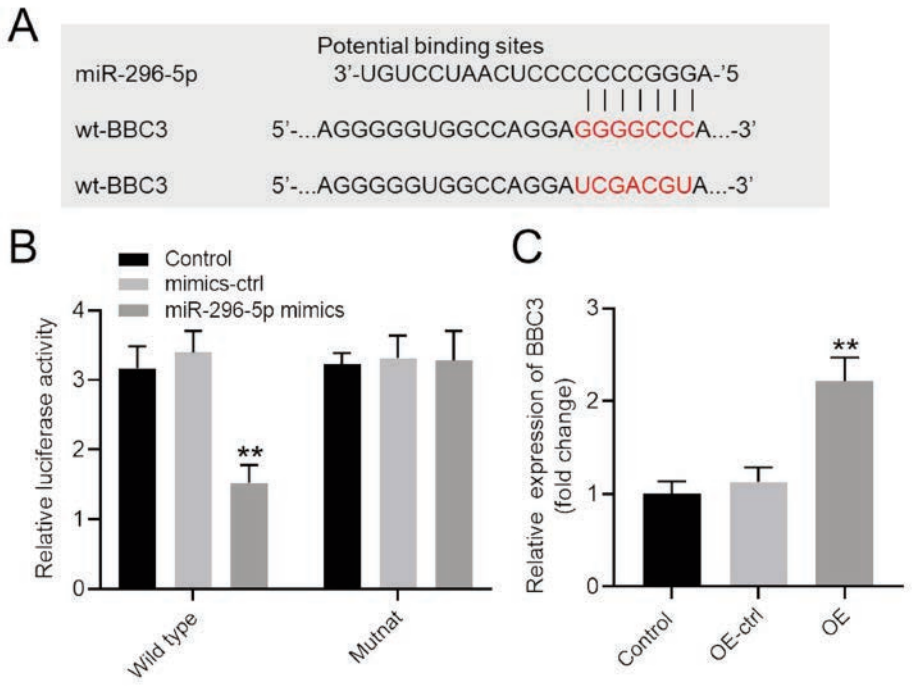

Figure 4. BBC3 was identified to be the downstream mRNA of miR-296-5p. **A**) Targetscan was used to predict the downstream mRNA of miR-296-5p.**B**) The luciferase activity was assessed by dual luciferase activity. **C**) Pulmonary fibroblasts were treated with pcDNA3.1 or pcDNA3.1-hsa_circ_0001861; the level of BBC3 in pulmonary fibroblasts was tested by RT-qPCR. **p<0.01 compared to control.

Hsa_circ_0001861 overexpression alleviates the progression of pulmonary fibrosis *in vivo*

To verify the function of hsa_circ_0001861 in pulmonary fibrosis, an *in vivo* model was constructed. As demonstrated in Figure 7 A,B, BLM significantly induced fibrosis and inflammatory infiltration in mice, which was markedly restored by hsa_circ_0001861 upregulation. Consistently, the BLM-induced upregulation of collagen I and α-SMA in mice was markedly abolished by hsa_circ_0001861 upregulation (Figure 7 C,D). In combination, the overexpression of hsa_circ_0001861 attenuated the progression of pulmonary fibrosis *in vivo*.

Discussion

It has been reported that pulmonary fibrosis manifests as an increase in internal fibrous connective tissue and a decrease in parenchymal cells.[34] The progression of oropharyngeal freezing could lead to the structural injury and dysfunction of organs.[35] CircRNAs have been shown to participate in pulmonary fibrosis. For example, Zhang *et al.* indicated that circ0044226 could regulate the lung myofibroblast transition and fibrosis;[36] circRNA homeodomain-interacting protein kinase 3 could modulate lung fibroblast-to-myofibroblast transition by binding to miR-338-3p.[14] In the present study, it was found that hsa_circ_0001861 was downregulated in TGF-β-treated pulmonary fibroblasts, and hsa_circ_0001861 overexpression could inhibit TGF-β-caused fibroblast proliferation and fibrosis by sponging miR-296-5p. Hence, the present study first investigated the function of hsa_circ_0001861 in pulmonary fibrosis and the mechanism underlying the function of hsa_circ_0001861 in pulmonary fibrosis, revealing that hsa_circ_0001861 may act as a key mediator in pulmonary fibrosis.

miRNAs were reported to be involved in lung fibrosis. For example, Rackow *et al* suggested that miR-338-3p could attenuate TGFβ-caused myofibroblast differentiation through the upregulation of phosphatase and tensin homolog;[37] Zhou *et al.* found that miR-302a-3p could promote the progression of pulmonary fibrosis by targeting tet methylcytosine dioxygenase 1.[38] Meanwhile, miR-296-5p was involved in the progression of fibrosis.[39] This study indicated that miR-296-5p could be sponged by hsa_circ_0001861

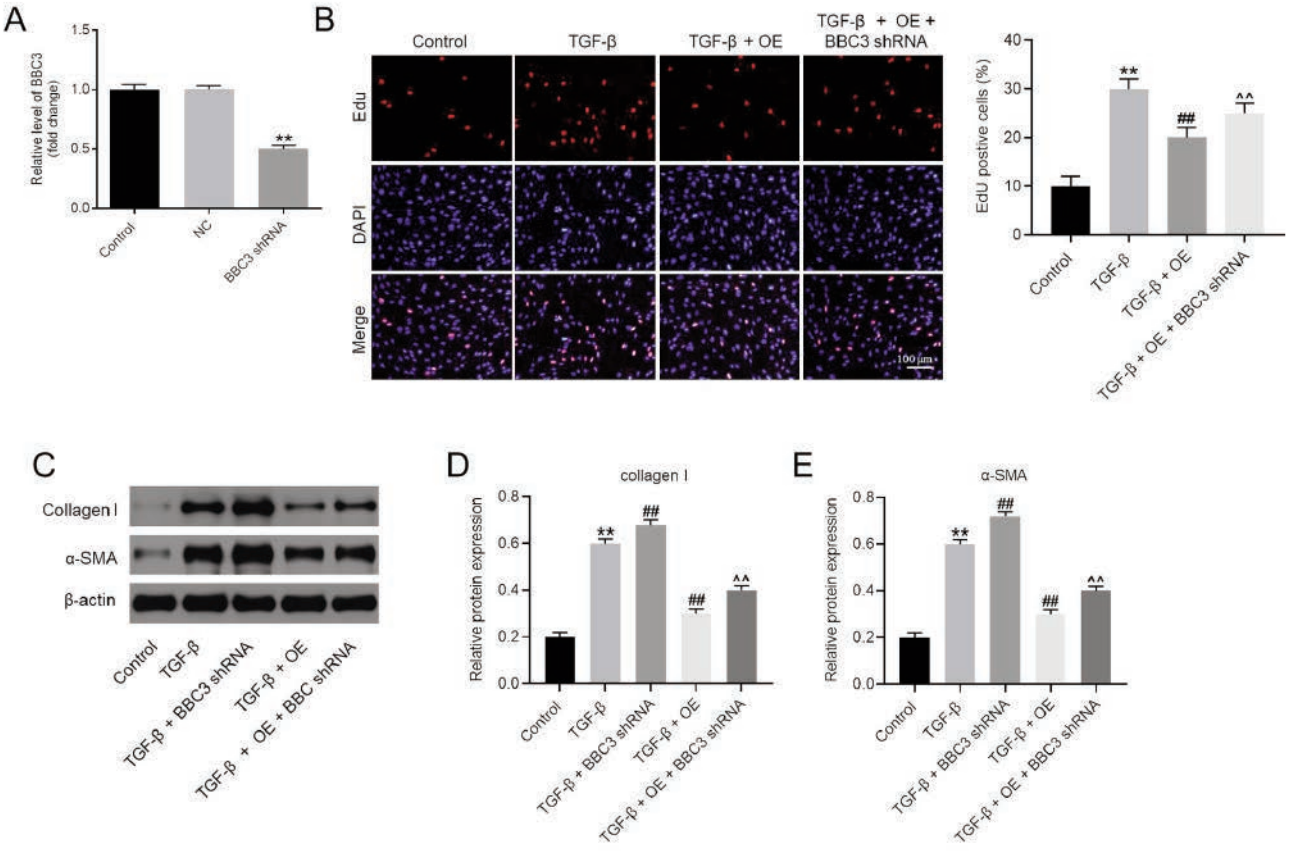

Figure 5. Hsa_circ_0001861 overexpression restored TGF-β-caused proliferation and fibrosis in fibroblasts *via* upregulation of BBC3. Pulmonary fibroblasts were transfected with BBC3 shRNA. **A**) The expression of BBC3 in pulmonary fibroblasts was tested by RT-qPCR; pulmonary fibroblasts were exposed to TGF-β, TGF-β + pcDNA3.1-hsa_circ_0001861 or TGF-β + pcDNA3.1-hsa_circ_0001861 + BBC3 shRNA. **B**) The proliferation of pulmonary fibroblasts was tested by EdU staining. **C-E**) Pulmonary fibroblasts were exposed to TGF-β, TGF-β + pcDNA3.1-hsa_circ_0001861, TGF-β + BBC3 shRNA or TGF-β + pcDNA3.1-hsa_circ_0001861 + BBC3 shRNA; the levels of α-SMA and collagen I in pulmonary fibroblasts were assessed by Western blot. **p<0.01 compared to control; ##p<0.01 compared to TGF-β; ^^p<0.01 compared to TGF-β + OE.

in pulmonary fibrosis. Therefore, this study first investigated the detailed role of miR-296-5p in pulmonary fibrosis. BBC3 plays crucial roles in cell behavior regulation.[40] In the present study, BBC3 was identified as the target of miR-296-5p. Hence, hsa_circ_0001861 could inhibit the progression of pulmonary fibrosis by modulating the miR-296-3p/BBC3 axis. On the other hand, Smad family member 2 (Smad2) and Smad3 are known to be key mediators in TGF-β signaling, and the phosphorylation of Smad2/Smad3 could lead to the progression of fibrosis.[41] Thus, the effect of hsa_circ_0001861 in TGF-β/Smad signaling needs to be confirmed soon. According to the previous reference, apoptosis could play an important role in pulmonary fibrosis.[42]

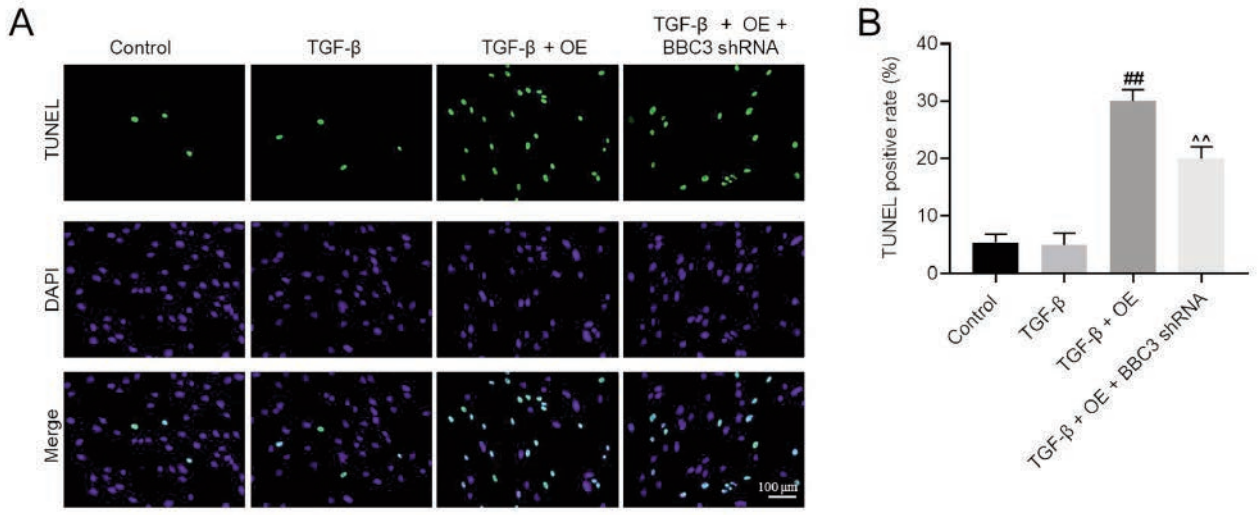

Figure 6. BBC3 knockdown reversed the apoptotic effect of hsa_circ_0001861 on TGF-β-treated fibroblasts. **A,B**) The apoptosis of fibroblasts was detected by TUNEL staining. ##p<0.01 compared to TGF-β; ^^p<0.01 compared to TGF-β + OE.

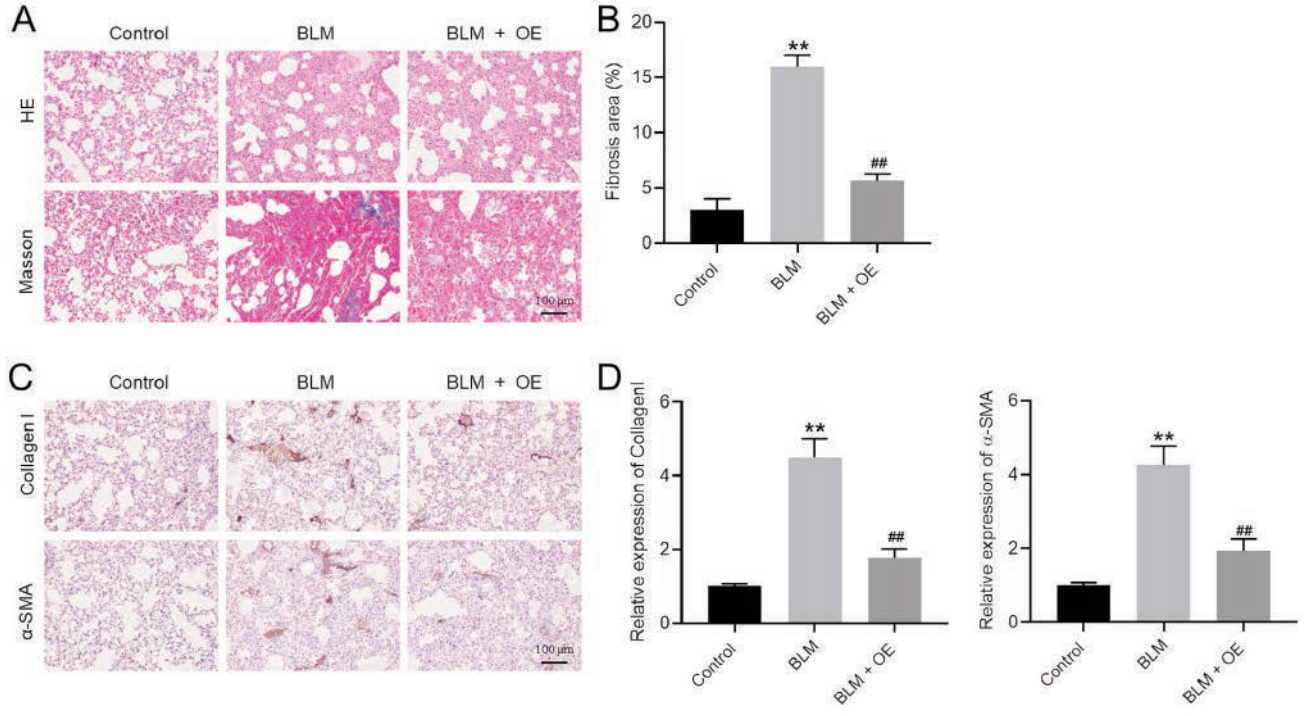

Figure 7. Overexpression of hsa_circ_0001861 attenuated the development of pulmonary fibrosis *in vivo*. **A,B**) The histological changes and fibrosis in tissues of mice were observed by H&E and Masson staining. **C,D**) The levels of α-SMA and collagen I in mice were investigated by immunohistochemistry staining. **p<0.01 compared to control; ##p<0.01 compared to BLM.

In addition, BBC3 could inhibit autophagy, and it could promote fibrosis through regulating autophagy.[33,43] Moreover, activation of autophagy could promote TGF-β-induced fibrosis through regulation of collagen I and α-SMA.[44,45] Thus, BBC3 knockdown could partially reverse the effect of hsa_circ_0001861 on fibrosis through inhibiting autophagy, and the mechanism by which BBC3 knockdown regulates the levels of collagen I and α-SMA will be investigated in coming future. This study was not without limitations. First, other miRNAs targeted by hsa_circ_0001861 in pulmonary fibrosis were not explored. Secondly, other targets of miR-296-5p in fibrosis were not investigated, and it is essential that they are studied in the future. Thirdly, the mechanism through which BBC3 knockdown regulates the levels of collagen I and α-SMA was not explored. In addition, the role of BBC3-mediated apoptosis in pulmonary fibrosis remains to be confirmed. Finally, BBC3 expression using specimens was missed. Hence, further analysis is essential in the future.

Hsa_circ_0001861 upregulation was found to attenuate bleomycin-induced pulmonary fibrosis progression in a mouse model, by indirectly targeting BBC3. Therefore, the present study may provide a new theoretical basis to clinicians for improving the treatment strategy against pulmonary fibrosis.

References

1. Li LC, Kan LD. Traditional Chinese medicine for pulmonary fibrosis therapy: Progress and future prospects. J Ethnopharmacol 2017;198:45-63.
2. Mudawi D, Heyes K, Hastings R, Rivera-Ortega P, Chaudhuri N. An update on interstitial lung disease. Br J Hosp Med (Lond) 2021;82:1-14.
3. He Y, Thummuri D, Zheng G, Okunieff P, Citrin DE, Vujaskovic Z, et al. Cellular senescence and radiation-induced pulmonary fibrosis. Transl Res 2019;209:14-21.
4. Yao MY, Zhang WH, Ma WT, Liu QH, Xing LH, Zhao GF. microRNA-328 in exosomes derived from M2 macrophages exerts a promotive effect on the progression of pulmonary fibrosis via FAM13A in a rat model. Exp Mol Med 2019; 51:63.
5. Shin YJ, Kim SH, Park CM, Kim HY, Kim IH, Yang MJ, et al. Exposure to cigarette smoke exacerbates polyhexamethylene guanidine-induced lung fibrosis in mice. J Toxicol Sci 2021;46:487-97.
6. Hatabu H, Kaye KM, Christiani DC. Viral infection, pulmonary fibrosis, and long COVID. Am J Respir Crit Care Med 2023;207:647-9.
7. Zhang Y, Liu Q, Ning J, Jiang T, Kang A, Li L, et al. The proteasome-dependent degradation of ALKBH5 regulates ECM deposition in PM(2.5) exposure-induced pulmonary fibrosis of mice. J Hazard Mater 2022;432:128655.
8. Feldman RM, Singer C. Noncardiogenic pulmonary edema and pulmonary fibrosis in falciparum malaria. Rev Infect Dis 1987;9:134-9.
9. Mishra S, Shah MI, Udhaya Kumar S, Thirumal Kumar D, Gopalakrishnan C, Al-Subaie AM, et al. Network analysis of transcriptomics data for the prediction and prioritization of membrane-associated biomarkers for idiopathic pulmonary fibrosis (IPF) by bioinformatics approach. Adv Protein Chem Struct Biol 2021;123:241-73.
10. Fang C, Huang H, Feng Y, Zhang Q, Wang N, Jing X, et al. Whole-exome sequencing identifies susceptibility genes and pathways for idiopathic pulmonary fibrosis in the Chinese population. Sci Rep 2021;11:1443.
11. Pang X, Shi H, Chen X, Li C, Shi B, Yeo AJ, et al. miRNA-34c-5p targets Fra-1 to inhibit pulmonary fibrosis induced by silica through p53 and PTEN/PI3K/Akt signaling pathway. Environ Toxicol 2022;37:2019-32.
12. Martinović Kaliterna D, Petrić M. Biomarkers of skin and lung fibrosis in systemic sclerosis. Expert Rev Clin Immunol 2019;15:1215-23.
13. Inoue Y, Kaner RJ, Guiot J, Maher TM, Tomassetti S, Moiseev S, et al. Diagnostic and prognostic biomarkers for chronic fibrosing interstitial lung diseases with a progressive phenotype. Chest 2020;158:646-59.
14. Zhang JX, Lu J, Xie H, Wang DP, Ni HE, Zhu Y, et al. circHIPK3 regulates lung fibroblast-to-myofibroblast transition by functioning as a competing endogenous RNA. Cell Death Dis 2019;10:182.
15. Kristensen LS, Hansen TB, Veno MT, Kjems J. Circular RNAs in cancer: opportunities and challenges in the field. Oncogene 2018;37:555-65.
16. Shan C, Zhang Y, Hao X, Gao J, Chen X, Wang K. Biogenesis, functions and clinical significance of circRNAs in gastric cancer. Mol Cancer 2019;18:136.
17. Yang L, Liu X, Zhang N, Chen L, Xu J, Tang W. Investigation of circular RNAs and related genes in pulmonary fibrosis based on bioinformatics analysis. J Cell Biochem 2019;120: 11022-32.
18. Li R, Wang Y, Song X, Sun W, Zhang J, Liu Y, et al. Potential regulatory role of circular RNA in idiopathic pulmonary fibrosis. Int J Mol Med 2018;42:3256-68.
19. Suzuki A, Sakamoto K, Nakahara Y, Enomoto A, Hino J, Ando A, et al. BMP3b is a novel anti-fibrotic molecule regulated by meflin in lung fibroblasts. Am J Respir Cell Mol Biol 2022;67:446-58.
20. Xu X, Ma C, Wu H, Ma Y, Liu Z, Zhong P, et al. Fructose induces pulmonary fibrotic phenotype through promoting epithelial-mesenchymal transition mediated by ROS-activated latent TGF-beta1. Front Nutr 2022;9:850689.
21. Lee JH, Lee CM, Lee JH, Kim MO, Park JW, Kamle S, et al. Kasugamycin is a novel chitinase 1 inhibitor with strong antifibrotic effects on pulmonary fibrosis. Am J Respir Cell Mol Biol 2022;67:309-19.
22. Aschner Y, Correll KA, Beke KM, Foster DG, Roybal HM, Nelson MR, et al. PTPalpha promotes fibroproliferative responses after acute lung injury. Am J Physiol Lung Cell Mol Physiol 2022;323:L69-L83.
23. Shi C, Chen X, Yin W, Sun Z, Hou J, Han X. Wnt8b regulates myofibroblast differentiation of lung-resident mesenchymal stem cells via the activation of Wnt/beta-catenin signaling in pulmonary fibrogenesis. Differentiation 2022;125:35-44.
24. Li J, Zhang X, Wang T, Li J, Su Q, Zhong C, et al. The MIR155 host gene/microRNA-627/HMGB1/NF-kappaB loop modulates fibroblast proliferation and extracellular matrix deposition. Life Sci 2021;269:119085.
25. Sun J, Su W, Zhao X, Shan T, Jin T, Guo Y, et al. LncRNA PFAR contributes to fibrogenesis in lung fibroblasts through competitively binding to miR-15a. Biosci Rep 2019;39BSR20 190280.
26. Ghahary A, Tredget EE, Chang LJ, Scott PG, Shen Q. Genetically modified dermal keratinocytes express high levels of transforming growth factor-beta1. J Invest Dermatol 1998;110:800-5.
27. Wang X, Zhao S, Lai J, Guan W, Gao Y. Anti-inflammatory, antioxidant, and antifibrotic effects of gingival-derived MSCs on bleomycin-induced pulmonary fibrosis in mice. Int J Mol Sci 2021;23:99.
28. Guan S, Liu H, Zhou J, Zhang Q, Bi H. The MIR100HG/miR-29a-3p/Tab1 axis modulates TGF-beta1-induced fibrotic changes in type II alveolar epithelial cells BLM-caused lung

fibrogenesis in mice. Toxicol Lett 2022;363:45-54.
29. Tassone P, Caruso C, White M, Tavares Dos Santos H, Galloway T, Dooley L, et al. The role of matrixmetalloproteinase-2 expression by fibroblasts in perineural invasion by oral cavity squamous cell carcinoma. Oral Oncol 2022;132:106002.
30. Zhang X, Qu H, Yang T, Liu Q, Zhou H. Astragaloside IV attenuate MI-induced myocardial fibrosis and cardiac remodeling by inhibiting ROS/caspase-1/GSDMD signaling pathway. Cell Cycle 2022;21:2309-22.
31. Meng XM, Nikolic-Paterson DJ, Lan HY. TGF-beta: the master regulator of fibrosis. Nat Rev Nephrol 2016;12:325-38.
32. Nakahara Y, Hashimoto N, Sakamoto K, Enomoto A, Adams TS, Yokoi T, et al. Fibroblasts positive for meflin have antifibrotic properties in pulmonary fibrosis. Eur Respir J 2021;58:2003397.
33. Fitzwalter BE, Thorburn A. FOXO3 links autophagy to apoptosis. Autophagy 2018;14:1467-8.
34. Guan R, Yuan L, Li J, Wang J, Li Z, Cai Z, et al. Bone morphogenetic protein 4 inhibits pulmonary fibrosis by modulating cellular senescence and mitophagy in lung fibroblasts. Eur Respir J 2022;60:2102307.
35. Duhig EE. Usual interstitial pneumonia: a review of the pathogenesis and discussion of elastin fibres, type II pneumocytes and proposed roles in the pathogenesis. Pathology 2022;54:517-25.
36. Zhang L, Chi X, Luo W, Yu S, Zhang J, Guo Y, et al. Lung myofibroblast transition and fibrosis is regulated by circ0044226. Int J Biochem Cell Biol 2020;118:105660.
37. Rackow AR, Judge JL, Woeller CF, Sime PJ, Kottmann RM. miR-338-3p blocks TGFbeta-induced myofibroblast differentiation through the induction of PTEN. Am J Physiol Lung Cell Mol Physiol 2022;322:L385-L400.
38. Zhou Y, Gao Y, Zhang W, Chen Y, Jin M, Yang Z. Exosomes derived from induced pluripotent stem cells suppresses M2-type macrophages during pulmonary fibrosis via miR-302a-3p/TET1 axis. Int Immunopharmacol 2021;99:108075.
39. Fang L, Ellims AH, Moore XL, White DA, Taylor AJ, Chin-Dusting J, et al. Circulating microRNAs as biomarkers for diffuse myocardial fibrosis in patients with hypertrophic cardiomyopathy. J Transl Med 2015;13:314.
40. Feng L, Chen X, Zhang S, Chen Y, Yu Y. Role of miR-139-5p in ectopic endometrial stromal cells and the underlying molecular mechanism. Exp Ther Med 2021;22:1251.
41. Shi W, Hao J, Wu Y, Liu C, Shimizu K, Li R, et al. Protective effects of heterophyllin B against bleomycin-induced pulmonary fibrosis in mice via AMPK activation. Eur J Pharmacol 2022;921:174825.
42. Kuwano K, Hagimoto N, Nakanishi Y. The role of apoptosis in pulmonary fibrosis. Histol Histopathol 2004;19:867-81.
43. Liu H, Cheng Y, Yang J, Wang W, Fang S, Zhang W, et al. BBC3 in macrophages promoted pulmonary fibrosis development through inducing autophagy during silicosis. Cell Death Dis 2017;8:e2657.
44. He R, Wang M, Zhao C, Shen M, Yu Y, He L, et al. TFEB-driven autophagy potentiates TGF-beta induced migration in pancreatic cancer cells. J Exp Clin Cancer Res 2019;38:340.
45. Liu N, Feng J, Lu X, Yao Z, Liu Q, Lv Y, et al. Isorhamnetin inhibits liver fibrosis by reducing autophagy and inhibiting extracellular matrix formation via the TGF-beta1/Smad3 and TGF-beta1/p38 MAPK pathways. Mediators Inflamm 2019;2019:6175091.

Received: 26 July 2023. Accepted: 29 August 2023.

Licensee PAGEPress, Italy
European Journal of Histochemistry 2023; 67:3839
doi:10.4081/ejh.2023.3839